

# Inhibition of Retinoblastoma In Vitro and In Vivo with Conditionally Replicating Oncolytic Adenovirus H101

Xin Song,<sup>1,2</sup> Yixiong Zhou,<sup>1,2</sup> Renbing Jia,<sup>1</sup> Xiaofang Xu,<sup>1</sup> Haibo Wang,<sup>3,4</sup> Jifan Hu,<sup>4</sup> Shengfang Ge,<sup>3</sup> and Xianqun Fan<sup>1</sup>

**PURPOSE.** To determine the therapeutic effect of oncolytic adenovirus H101 on retinoblastoma in vitro and in vivo.

**METHODS.** The expression of coxsackievirus-adenovirus receptor (CAR) in human retinoblastoma cell line HXO-RB<sub>44</sub> was determined by RT-PCR, Western blot, immunofluorescence, and immunocytochemistry staining. Appropriate multiplicity of infection was determined using flow cytometry in retinoblastoma cells with green fluorescent protein-expressing adenovirus (AdGFP). The viability of HXO-RB<sub>44</sub> cells treated with H101 or AdGFP was measured using a cell counting kit-8-based procedure. Viral proliferation in vitro was measured by end point dilution titration and real-time PCR. Cell cycle and apoptotic activity of HXO-RB<sub>44</sub> were analyzed by flow cytometry. NOD-SCID mice bearing retinoblastoma xenografts were treated with intratumoral injection of H101, AdGFP, or PBS. Tumor volume and survival time were recorded. Immunohistochemistry for adenoviral fiber protein and Western blot for adenoviral Hexon protein of retinoblastoma xenografts were performed to evaluate H101 virus replication in vivo.

**RESULTS.** HXO-RB<sub>44</sub> cells expressed CAR and were sensitive to adenoviral infection. HXO-RB<sub>44</sub> cells treated with H101 had reduced cell viability compared with AdGFP-treated cells ( $P < 0.01$ ). Abundant replication of H101 in HXO-RB<sub>44</sub> cells resulted in G<sub>2</sub>/M-phase arrest and finally tumor cell lysis, but the apoptosis pathway was not activated. Tumor-bearing mice treated with H101 had reduced tumor burdens and prolonged survival times compared with PBS and AdGFP controls (both  $P < 0.01$ ). Immunohistochemical and Western blot examination revealed widespread replication of H101 within the tumor.

**CONCLUSIONS.** These results suggest that H101 effectively inhibits the growth of retinoblastoma cells in vitro and in mice and

may serve as a novel therapy for retinoblastoma. (*Invest Ophthalmol Vis Sci.* 2010;51:2626–2635) DOI:10.1167/iovs.09-3516

Retinoblastoma is the most common childhood primary intraocular malignant tumor.<sup>1</sup> It is estimated that 5000 new cases of retinoblastoma are diagnosed worldwide each year.<sup>2</sup> In the United States, the overall mean age-adjusted incidence of retinoblastoma is 11.8 per million children between birth and 4 years.<sup>3</sup>

The primary goal of treatment for retinoblastoma is to save the patient's life, and the secondary goal is to save the eyeball and the patient's vision if possible. Enucleation, a successful approach to treat intraocular retinoblastoma as first published in 1809, is now the standard therapy for patients with advanced intraocular disease.<sup>4</sup> Enucleation can cure unilateral disease in more than 95% of patients but may result in vision loss and an unsatisfactory cosmetic appearance.<sup>5</sup>

Numerous alternative treatment modalities are now being used for retinoblastoma, including thermotherapy, cryotherapy, external beam radiotherapy, chemotherapy (systemic and local delivery), and brachytherapy. The choice of treatment is determined largely by the size, location, and laterality of the tumor and by the vision potential and age of the child.<sup>6</sup> Thermotherapy and cryotherapy are only useful for small lesions without vitreous seeding; external beam radiotherapy may result in severe complications and can increase the risk for secondary malignant tumor; chemotherapy is commonly used to reduce tumor size before administration of local therapy. Recent studies suggest that adjuvant chemotherapy may effectively reduce the incidence of metastases in patients who have retinoblastoma with massive choroidal invasion or postlaminar optic nerve invasion.<sup>7,8</sup> Eyes with diffuse vitreous seeding, however, present a particularly difficult management problem and rarely respond to chemotherapy alone.<sup>9</sup> Therefore, new modalities are needed to save affected eyes without later life-threatening consequences.

A virus-based strategy takes advantage of the fact that the replication and production of adenoviral progeny require the cell cycle gatekeeper *p53* to be in an inactive status, which is commonly observed in tumors caused by mutation or epigenetic silencing of the gene. One viral early gene, *E1B*, which encodes a 55-kDa protein (*E1B 55K*), is essential to virus replication. *E1B* interacts with cellular *p53* and inactivates it to allow viral replication. ONYX-015, a modified adenovirus that lacks the *E1B 55K* gene, can only replicate and lyse tumor cells that have inactivated *p53*, sparing normal cells that retain wild-type *p53* function.<sup>10</sup> Clinical trials in patients with recurrent head and neck cancer, metastatic colorectal cancer, or pancreatic cancer have shown that ONYX-015, used either alone or in combination with chemotherapy, is safe and has significant antitumor effect in at least a fraction of the patients.<sup>11–13</sup>

In China, an oncolytic adenovirus called H101 has been clinically approved for the treatment of several malignancies.<sup>14</sup>

From the <sup>1</sup>Department of Ophthalmology, Ninth People's Hospital, Shanghai Jiao Tong University School of Medicine, Shanghai, P. R. China; the <sup>2</sup>Department of Biochemistry and Molecular Biology, Shanghai Jiao Tong University School of Medicine, Shanghai, P. R. China; and <sup>4</sup>VA Palo Alto Health Care System, Stanford University Medical School, Palo Alto, California.

<sup>3</sup>These authors contributed equally to the work presented here and should therefore be regarded as equivalent authors.

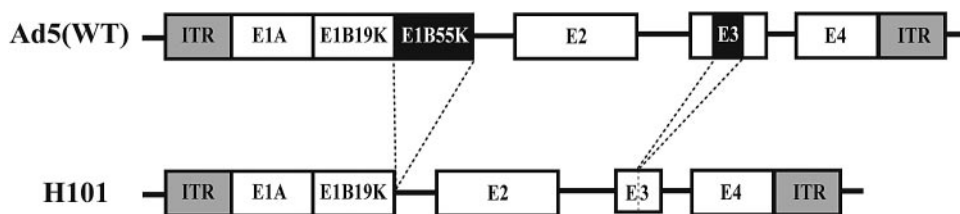
Supported by National Natural Science Foundation of China Grants 30973663 and 10935009; Shanghai Leading Academic Discipline Project Grant S30205; and Science and Technology Commission of Shanghai Grants 064119537, 07JC14034, and 08410702300.

Submitted for publication February 4, 2009; revised October 14 and November 23, 2009; accepted November 24, 2009.

Disclosure: X. Song, None; Y. Zhou, None; R. Jia, None; X. Xu, None; H. Wang, None; J. Hu, None; S. Ge, None; X. Fan, None

Corresponding author: Xianqun Fan, Department of Ophthalmology, Ninth People's Hospital, Shanghai Jiao Tong University School of Medicine, NO.639 Zhi Zao Ju Road, Shanghai, 200011, P. R. China; fanxq@sh163.net.

**FIGURE 1.** Construction of the H101 oncolytic virus. The cellular *p53* protein blocks viral replication. In the wild-type adenovirus 5, *E1B 55K* protein binds to and inactivates *p53* to allow viral replication. In the H101 adenovirus, deletion of the *E1B 55K* gene (black box) allows it to be replicated only in tumor cells that have the inactivated *p53*, whereas normal cells that retain wild-type *p53* function are spared. Compared with the wild-type Ad5, part of the *E3* (black box) that encodes the adenovirus death protein was also deleted in H101.



Both *E1B* and parts of the *E3* regions are deleted in this virus. Without *E1B* to inactivate *p53*, H101 adenovirus cannot replicate and lyse normal cells where *p53* is active. Deletion of a 78.3- to 85.8- $\mu$ m gene segment in the *E3* region, which includes the adenovirus death protein, may enhance the safety of the product.<sup>14</sup> Thus, H101 can selectively infect—and kill—tumor cells through viral oncolysis.<sup>15</sup> However, therapeutic application of H101 in retinoblastomas has not been documented.

In human solid tumors, *p53* is inactivated by genetic mutation of the *Tp53* gene.<sup>16</sup> However, in retinoblastomas, the *p53* pathway is frequently inactivated through the amplification of *MDMX* and *MDM2*, which inhibit *p53* activity by multiple mechanisms.<sup>17,18</sup> It is estimated that the *p53* pathway is inactivated in 75% of retinoblastoma patients because of overexpressed *MDM2* and *MDMX* genes.<sup>19</sup> We thus reasoned that the H101 oncolytic adenovirus that targets *p53* inactivation in tumors might also work as a potential therapy for patients with retinoblastoma.

In the present study, we examined whether treatment with H101 oncolytic adenovirus inhibits the growth of retinoblastoma in vitro and in vivo. Our findings support the potential of H101 oncolytic therapy in treatment of retinoblastoma.

## MATERIALS AND METHODS

### Oncolytic Adenoviruses

H101, provided by Shanghai Sunway Biotech (Shanghai, China), was a recombinant human group C adenovirus with the deletion of the *E1B* region that encodes a 55-kDa protein and partial deletion of a 78.3- to 85.8- $\mu$ m-long gene segment in the *E3* region that encodes the adenovirus death protein (Fig. 1). Without *E1B*, H101 selectively infects and lyses tumor cells. Control AdGFP (Vector Gene Technology Company Ltd., Beijing, China) was an *E1*-deleted replication-deficient adenovirus in which the reporter of enhanced green fluorescent protein (GFP) was inserted into the *E1* region under control of the cytomegalovirus promoter.

### Cell Line and Cell Culture

Human retinoblastoma cell line HXO-RB<sub>44</sub> (kindly provided by Zhu Heping, Zhongnan University, Wuhan, China) was cultured in RPMI 1640 with 10% fetal bovine serum. HEK293 human embryonic kidney cells (HEK293) from the American Type Culture Collection (Manassas, VA) were cultured in Dulbecco's modified Eagle's medium supplemented with 10% fetal bovine serum.

### Reverse Transcription-Polymerase Chain Reaction

Total RNA was extracted from HXO-RB<sub>44</sub> and HEK293 using reagent (TRIzol; Invitrogen, Carlsbad, CA) according to the manufacturer's protocol. Briefly, 3  $\mu$ g RNA was reverse-transcribed in a 20- $\mu$ L reaction volume containing 0.5 mM dNTPs, 2.5  $\mu$ M random primers, 40 U RNase inhibitor, and 200 U M-MLV reverse transcriptase (Invitrogen). Reactions were performed for 10 minutes at 25°C, 40 minutes at 37°C, and 15 minutes at 70°C, followed by cooling to 4°C. The cDNA

samples were subjected to PCR using specific primers for the coxsackievirus-adenovirus receptor (CAR): 5'-TTGCTTGCTCTAGCGCTCATTGGT C-3' (forward); 5'-TCATCACAGGAATCGCACCCATTTCG-3' (reverse). Primers for *GAPDH* were 5'-AATCCCATCACCATTCTCC-3' (forward) and 5'-AGTCCTTCCACGATACCAA-3' (reverse). PCR reaction mixtures contained 1  $\mu$ L cDNA, 1.5 mM MgCl<sub>2</sub>, 0.2 mM dNTP, and 0.5  $\mu$ M primers. The following reaction cycle was performed 35 times: 95°C, 30 seconds; 58°C, 30 seconds; 72°C, 45 seconds. PCR products were separated by electrophoresis on 2% agarose gels, stained with ethidium bromide, and visualized under UV light.

### Immunofluorescence Detection of CAR

HXO-RB<sub>44</sub> cells were collected and blocked with normal horse serum (1:50 dilution in PBS with 0.5% bovine serum albumin [BSA]; Vector, Burlingame, CA) at 37°C for 30 minutes. After they were washed with PBS twice, cells were incubated with mouse monoclonal antibodies recognizing CAR (1:50 dilution in PBS/0.5% BSA; Santa Cruz Biotechnology, Santa Cruz, CA) at 37°C for 2 hours. Cells were washed with PBS twice, incubated with goat anti-mouse IgG secondary antibody (DyLight 488; 1:200 dilution in PBS/0.5% BSA; BD Biosciences, San Diego, CA) and propidium iodide (PI; 1:1000 dilution in PBS; Sigma-Aldrich, St. Louis, MO). Cells were placed on coverslips and photographed with a fluorescence microscope at 490 to 520 nm.

### Immunocytochemistry Detection of CAR

HXO-RB<sub>44</sub> cells were collected and attached to glass slides with cytospin centrifugation (Cytospin 4 Cyto centrifuge; Thermo, Shanghai, China). Cells were fixed with cold 95% acetone for 30 minutes, washed with PBS twice, and incubated with 0.25% Triton X-100, 5% dimethyl sulfoxide in PBS for 10 minutes. After incubation with 1.5% hydrogen peroxide for 10 minutes and two washes in PBS, cytospin slides were blocked with normal horse serum (1:50 dilution in PBS with 0.5% BSA; Vector) at 37°C for 30 minutes and incubated with mouse monoclonal antibodies recognizing CAR (1:50 dilution in PBS/0.5% BSA; Santa Cruz Biotechnology) at 4°C overnight. This was followed by the biotinylated anti-mouse IgG (Vectastain ABC Kit; Vector) at a 1:500 dilution for 30 minutes at 37°C. After two washes with PBS, slides were subsequently incubated with avidin-biotin-peroxidase complex (Vectastain ABC Kit; Vector) and diaminobenzidine substrate to develop the colorimetric reaction. Nuclear counterstaining was performed with hematoxylin for 2 minutes.

### Infectivity Assay

AdGFP was used to evaluate the infectivity of H101 in HXO-RB<sub>44</sub> cells. Short-term cultures of HXO-RB<sub>44</sub> (10<sup>5</sup> cells/well in a 24-well plate) in triplicate were incubated with AdGFP at 1, 10, 100, and 1000 multiplicities of infection (MOI) for 2 hours. Cells were harvested 48 hours later and analyzed (FACSCalibur; Becton Dickinson, Franklin Lakes, NJ).

### Cell Viability Assay

HXO-RB<sub>44</sub> cells were plated at a density of 1  $\times$  10<sup>4</sup> cells per well in a 96-well plate. After incubation for 6 hours, H101 was added to each well at an MOI of 1, 10, 100, and 1000. Cells treated with PBS or AdGFP

(MOI 100) were used as negative or positive control. Cell viability was quantified using a cell counting kit-8 (CCK-8; Dojindo, Kumamoto, Japan) for 5 consecutive days after infection. Viability was defined as follows:

$$\text{Viability} = \frac{A_{\text{experimental}} - A_{\text{background}}}{A_{\text{control}} - A_{\text{background}}} \times 100\%$$

where  $A_{\text{experimental}}$  is the absorbance of the experimental sample,  $A_{\text{control}}$  is the absorbance of the control sample, and  $A_{\text{background}}$  is the absorbance of the medium. Each data point was obtained in triplicate. Pictures were taken on day 5 to compare cell morphology among three treatment groups.

### In Vitro Adenovirus Replication Assay

HXO-RB<sub>44</sub> cells were cultured on six-well plates and were infected with H101 or AdGFP at an MOI of 100. Four hours after infection, the cells were washed with PBS to remove any free virus in the medium. Cells and supernatant were harvested 24, 48, and 72 hours after infection, and cell lysates were prepared by three cycles of freezing and thawing. Virus titers were determined by end point dilution titration on HEK293 cells.

### Real-Time PCR

HXO-RB<sub>44</sub> cells were harvested at 24, 48, and 72 hours after infection with H101 (MOI 100). Total RNA was extracted and reverse-transcribed into cDNA as described previously.<sup>20</sup> SYBR real-time PCR of Hexon protein mRNA was performed according to the manufacturer's instructions (TaKaRa, Tokyo, Japan). Specific PCR primers for Hexon protein were 5'-TAACCAGTCACAGTCGCAAG-3' (forward) and 5'-GTCAAAGTACGTG-GAAGCCAT-3' (reverse). After the denaturation step at 95°C for 10 seconds, the amplification program was set at 40 cycles, consisting of 95°C for 15 seconds, 59°C for 30 seconds, and 72°C for 30 seconds per cycle. Reactions were performed, and the data were analyzed (Rotor Gene 2000; Qiagen, Valencia, CA). Results were analyzed by comparing  $2^{-\Delta\Delta C_t}$  values of Hexon mRNA in adenovirus-infected cells and controls.

### Cell Cycle

Cells were harvested at 24, 48, and 72 hours after infection with H101 (MOI 100), fixed in 100% chilled ethanol, and kept at -20°C for at least 24 hours. To measure DNA content, cells were washed twice with PBS and stained with 25 µg/mL PI (Sigma-Aldrich). Cell cycle distribution was determined by flow cytometry analysis. Ten thousand events were acquired for each sample and analyzed.

### Apoptotic Analysis

Apoptosis was analyzed by flow cytometry using dual staining with annexin-V-fluorescein isothiocyanate and PI. Cells were prepared according to the manufacturer's instruction provided by the Annexin V-FITC apoptosis kit (BD Biosciences). Apoptosis was quantified on a fluorescence-activated cell sorter (Becton Dickinson, Sunnyvale, CA), and data from 10,000 events were collected for further analysis.

### Animal Studies

Animal studies were performed in accordance with the ARVO Statement for the Use of Animals in Ophthalmic and Vision Research in a protocol approved by Shanghai Jiao Tong University. HXO-RB<sub>44</sub> tumor xenografts were established by subcutaneous injection of  $5 \times 10^7$  cells into the right flanks of 4- to 6-week-old male NOD-SCID mice. When tumors reached the required mean tumor volume (100-200 mm<sup>3</sup>) as determined by the formula volume = length  $\times$  width<sup>2</sup>  $\times$  0.5, animals were randomly assigned into three groups (eight mice per group). The H101 group received intratumoral injections of H101 at  $1 \times 10^8$  pfu for 4 consecutive days; the AdGFP group received four infections with AdGFP; and control group mice were injected with PBS in an equivalent volume and schedule. Tumor size was measured by vernier callipers every 4 days.

In tumor survival study (eight mice per group), mice were euthanized in accordance with our animal protocol, when the tumor size reached >1000 mm<sup>3</sup>, suggesting that the mice would die within 1 week. Animal survival was recorded on the basis of the date of euthanization.

### Immunohistochemistry for Adenoviral Fiber Protein

Mice from each group were selected randomly and killed on day 7 after treatment for immunohistochemical staining. Tumor, neighboring muscle, kidney, liver, heart, lung, and spleen samples were taken, fixed in 10% formalin, and embedded in paraffin, and 4-µm sections were cut. Tumor sections were incubated at 4°C overnight with a mouse anti-adenovirus fiber antibody (Abcam, Boston, MA) at a dilution of 1:500. Sections were rinsed in PBS-T (0.05% Triton X-100 in PBS), followed by the biotinylated goat anti-mouse secondary antibody at a 1:500 dilution for 1 hour at room temperature. After two washes with PBS-T, slides were incubated with streptavidin-horseradish peroxidase (Dako, Glostrup, Denmark) and diaminobenzidine substrate to develop the colorimetric reaction. All slides were counterstained with hematoxylin. Adenoviral positive HXO-RB<sub>44</sub> cells were quantitated (QWin Plus; Leica, Wetzlar, Germany) and calculated as the percentage for each treatment group.

### Western Blot Analysis for CAR and Hexon Protein

HXO-RB<sub>44</sub> cells and HEK293 cells were harvested and used for CAR analysis. Proteins were separated by sodium dodecyl sulfate-polyacrylamide gel electrophoresis in 12% (wt/vol) polyacrylamide gels and transferred to polyvinylidene fluoride membranes. Membranes were incubated with secondary antibody conjugated to a fluorescent tag; the bands were visualized and quantified by an infrared imaging system (Odyssey; LI-COR, Lincoln, NE). The antibodies used were CAR (Abcam) and β-actin (Santa Cruz Biotechnology).

Mice from each group were selected randomly and killed on day 14 after treatment. Tumors were homogenated in liquid nitrogen. Viral Hexon proteins were quantitated by Western blot analysis, as previously described. Antibodies used were Hexon (Abcam) and GAPDH (Santa Cruz Biotechnology).

### Statistical Analysis

All experiments were performed in triplicate, and the data were expressed as mean  $\pm$  SD. The data were analyzed with Student's *t*-test, and results were considered statistically significant at  $P \leq 0.05$ .

## RESULTS

### Sensitivity of HXO-RB<sub>44</sub> to Adenovirus Infection

CAR has a crucial role in adenoviral infection and may be important in the sensitivity of retinoblastoma toward H101. CAR gene and protein expression in HXO-RB<sub>44</sub> was examined by RT-PCR and Western blot analysis. The HEK293 cells were used as positive controls. As shown in Figures 2A and 2B, CAR was present in HXO-RB<sub>44</sub> cells. Both immunocytochemistry staining and immunofluorescence staining also confirmed CAR protein expression on the cell membranes of HXO-RB<sub>44</sub> cells (Figs. 2C, 2D).

Using an adenovirus expressing GFP under the cytomegalovirus promoter (AdGFP), we examined the infection efficiency of retinoblastoma cells by flow cytometry analysis (Fig. 2E). HXO-RB<sub>44</sub> cells exhibited a significant increase in the percentage of cells expressing GFP at an MOI as low as 10 pfu/cell, demonstrating their high sensitivity to adenoviral infection. The infection efficiency of the HXO-RB<sub>44</sub> was 82% at an MOI of 100 pfu/cell and did not significantly increase further at a higher MOI. These findings suggest that a dose of 100 pfu/cell produces optimal infectivity in vitro.

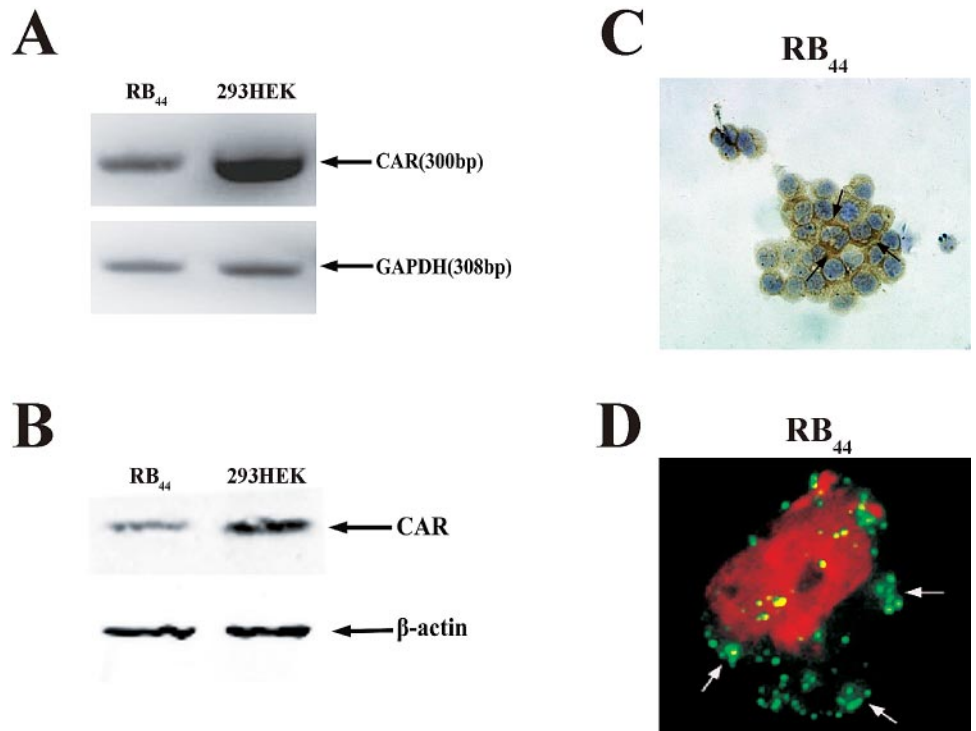


**FIGURE 2.** HXO-RB<sub>44</sub> cells are positive for CAR and are sensitive to adenoviral infection. (A) HXO-RB<sub>44</sub> was analyzed by RT-PCR using specific primers for CAR mRNA. The HEK293 cells were used as a positive control. (B) Western blot analysis of CAR protein expression. (C) Immunohistochemical staining of CAR in HXO-RB<sub>44</sub> cells. Nuclei were counterstained with hematoxylin (blue), and CAR was visualized with diaminobenzidine (brown; black arrows). (D) Immunofluorescence detection of CAR in HXO-RB<sub>44</sub> cells. Nuclei were stained with PI (red), and CAR was visualized with goat anti-mouse IgG secondary antibody (green; white arrows). Original magnification,  $\times 400$ . (E) Infectivity of retinoblastoma tumor cells with AdGFP. Tumor cells were incubated in culture conditions and infected with AdGFP at 1, 10, 100, and 1000 pfu/cells. GFP values represent three independent experiments (mean  $\pm$  SD;  $n = 3$ ; \* $P < 0.05$ , \*\* $P < 0.01$ , compared with infectivity of 1 pfu/cell group).

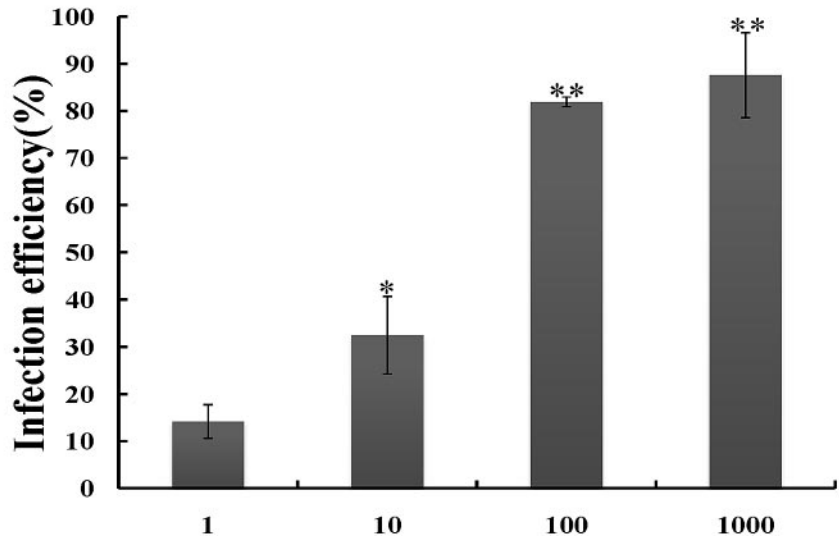
**Cytotoxicity of H101 In Vitro**

The ability of H101 to kill retinoblastoma cells was assessed with an assay kit (CCK-8). We treated HXO-RB<sub>44</sub> cells with H101 at various MOIs ranging from 1 to 1000 pfu/cell. Cells treated with PBS or AdGFP were used as negative or positive control, respectively. Based on the dose-time response curve shown in Figure 3A, HXO-RB<sub>44</sub> cells had nearly 20% cell viability 5 days after infection at an MOI of 100. Cell viability was reduced to similar levels when infected with a higher MOI. These results were consistent with infection efficacy data and confirmed that a dose of 100 pfu/cell was optimal for treatment in vitro. HXO-RB<sub>44</sub> cells treated with H101 dramatically reduced cell viability compared with AdGFP at the same MOIs

( $P < 0.01$ ; Fig. 3B). Under an inversion microscope, HXO-RB<sub>44</sub> cells were healthy in both the AdGFP group and the PBS group but were obviously lytic in the H101 group (see Fig. 6B).

**H101 Replication In Vitro**

To determine H101 replication in retinoblastoma in vitro, we performed end point dilution titration on HEK293 cells. H101 replication was highly efficient in HXO-RB<sub>44</sub> cells, with a replication index of 400 (i.e., every virus gave rise to 400 progeny viruses within 48 hours; Fig. 4A). To further investigate H101 replication, we measured adenoviral late Hexon gene expression in a time-course experiment using HXO-RB<sub>44</sub> cells that were infected at an MOI of 100 at 24,



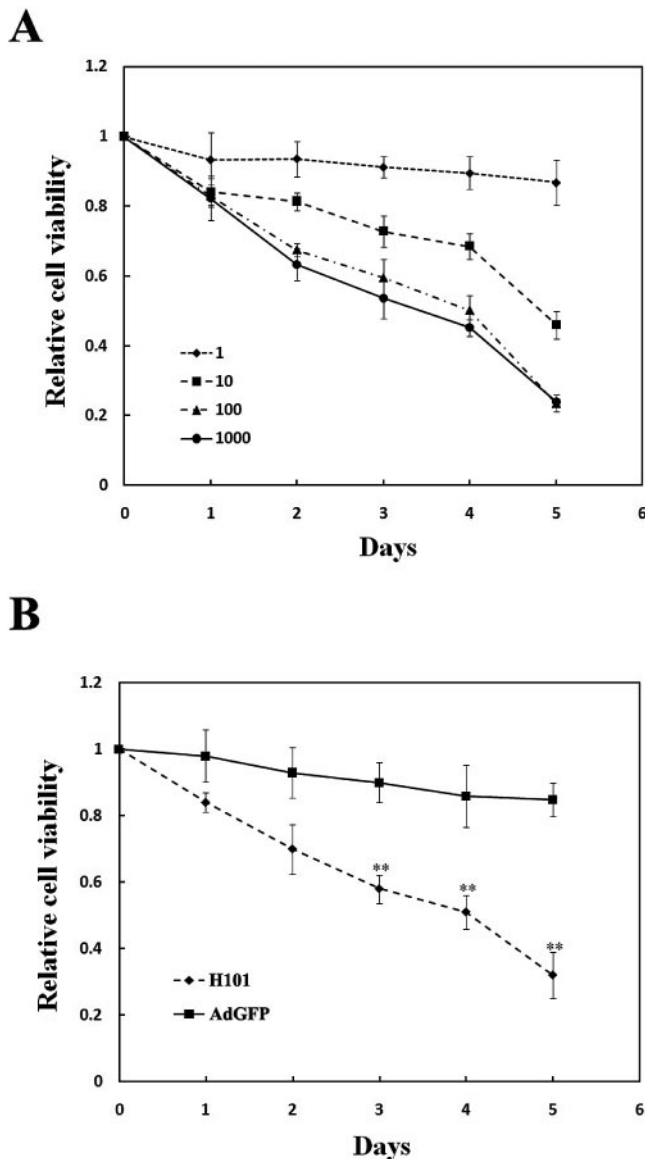


**FIGURE 3.** Cell viability assay. (A) HXO-RB<sub>44</sub> was treated with H101 at an MOI of 1, 10, 100, and 1000 pfu/cell for 120 hours. Cells treated with PBS were used as negative controls. (B) Cells treated with AdGFP (MOI 100) were used as positive controls. HXO-RB<sub>44</sub> treated with H101 dramatically reduced cell viability compared with AdGFP at the same MOIs. Cell viability was analyzed using the CCK-8 assay kit. The data represent three independent experiments (mean  $\pm$  SD;  $n = 3$ ; \*\* $P < 0.01$ , compared with HXO-RB<sub>44</sub> cells treated with AdGFP).

48, and 72 hours after infection. Hexon gene expression was strongly increased at 48 hours, followed by a further increase peak at 72 hours (Fig. 4B), thus confirming the end point dilution titration data.

### Inducement of G<sub>2</sub>/M-Phase Arrest in HXO-RB<sub>44</sub>

As an initial step to address the mechanism underlying H101 oncolysis in our retinoblastoma model, we analyzed the effect of H101 on the HXO-RB<sub>44</sub> cell cycle. We measured the cell cycle phase distribution by flow cytometry on samples stained with PI (Fig. 5). The results showed that H101 induced a significant accumulation of cells in G<sub>2</sub>/M, which occurred at 48 to 72 hours after infection in the H101 group.

### Effect of H101 on Apoptotic Pathway in HXO-RB<sub>44</sub>

We then analyzed whether H101 treatment led to tumor cell apoptosis. Twenty-four hours after infection, apoptosis was measured using an Annexin V-FITC apoptosis kit and flow cytometric analysis. As seen in Figure 6A, H101 at an MOI of 100 did not induce apoptosis in HXO-RB<sub>44</sub> cells (5.85%) compared with PBS control (4.20%), suggesting that cell apoptosis is not the major pathway by which H101 kills retinoblastoma cells. In contrast, though neither AdGFP nor PBS affected HXO-RB<sub>44</sub> cells, H101 caused extensive cell lysis in treated cells (Fig. 6B). Collectively, these data suggest that, as in other tumor models, H101 selectively induces tumor cell lysis in HXO-RB<sub>44</sub> retinoblastoma cells.

### Inhibition of Tumor Growth and Prolongation of Mouse Survival In Vivo by Treatment with H101

We tested the therapeutic efficacy of H101 in vivo in a human retinoblastoma xenograft mouse model. H101 significantly inhibited tumor growth compared with AdGFP and PBS ( $P < 0.01$ ; Fig. 7A). In contrast, AdGFP had no significant effect on tumor growth compared with the PBS-treated group ( $P > 0.05$ ; Fig. 7A). This result is consistent with the cytotoxicity data and virus replication data. As expected, no significant side effects were observed in animals at the end of the experiment.

The long-term therapeutic effect of H101 was examined by measuring animal survival in each treatment group. Mouse survival data indicated that those treated with H101 had a prolonged survival time; mean survival time was 31.1 days compared with 14.9 days for AdGFP and 11.5 days for PBS (Fig. 7B).

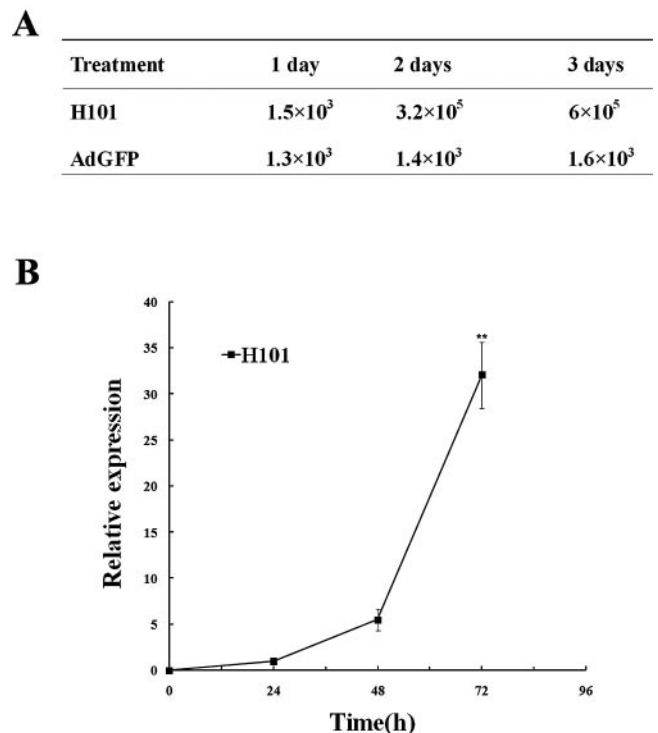


**FIGURE 4.** In vitro adenovirus replication assay. (A) The viral titers in HXO-RB<sub>44</sub> cells after treatment with H101 at an MOI of 100 for 24, 48, and 72 hours. (B) Viral DNA replication was determined by real-time PCR quantification of adenoviral late Hexon gene expression at 24 hours, 48 hours, and 72 hours after treatment with H101. For comparison, the mRNA expression of Hexon at 24 hours was arbitrarily defined as 1, and *GAPDH* was used as an internal control (\*\* $P < 0.01$ , compared with mRNA expression of Hexon at 48 hours).

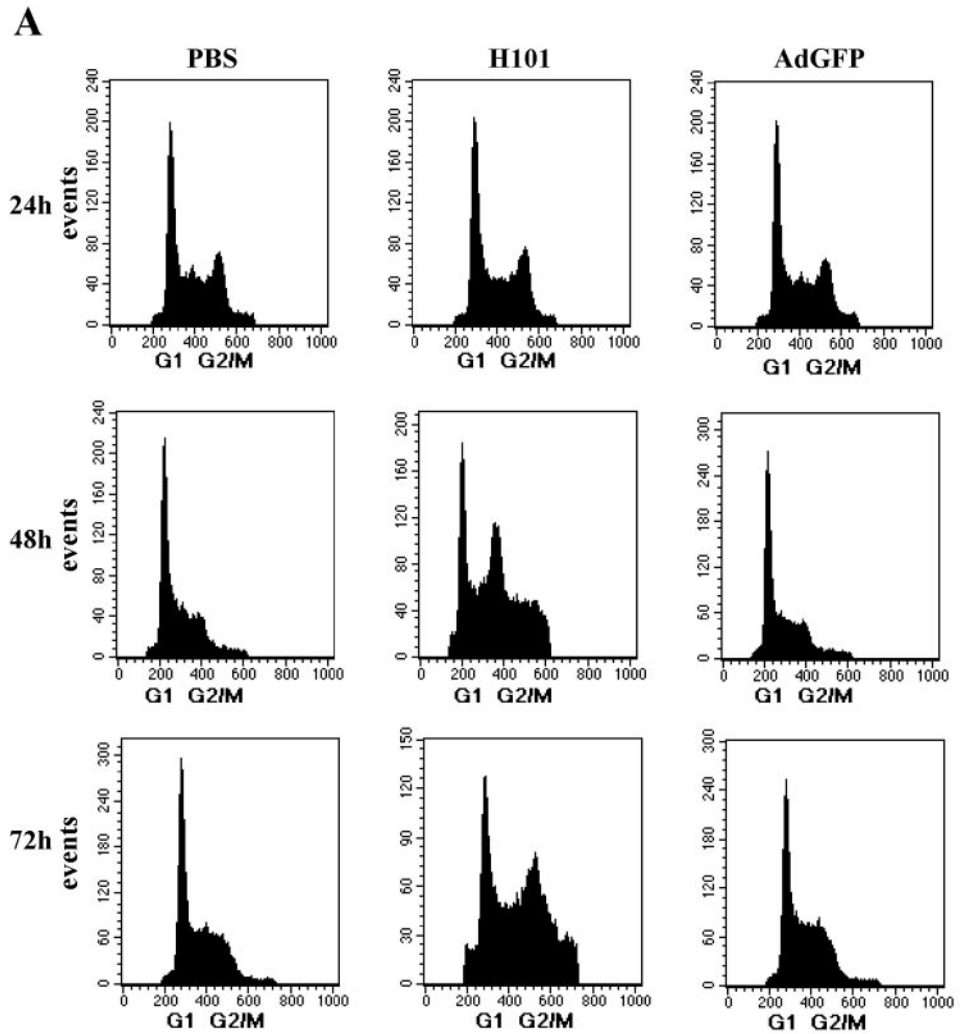
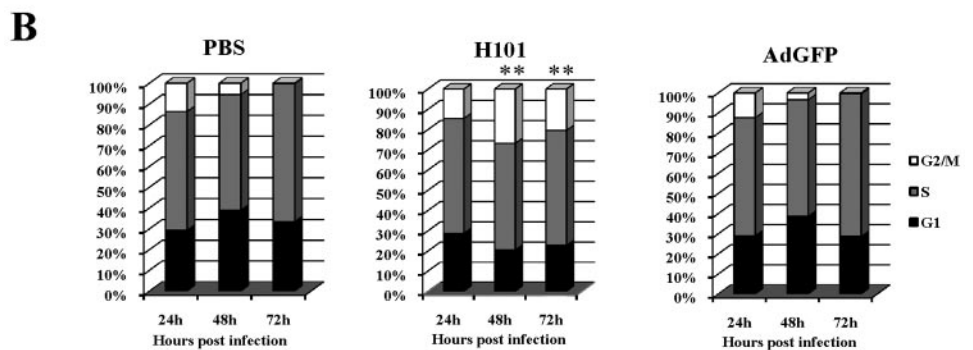


**FIGURE 5.** H101 induces G<sub>2</sub>/M arrest. HXO-RB<sub>44</sub> cells were infected with the indicated adenovirus at an MOI of 100. **(A)** Cell cycle analysis was performed by quantifying propidium iodide incorporation by flow cytometry. DNA content and number of events were analyzed at different times after infection. **(B)** Relative changes in percentage of cell cycle phase plotted at the indicated times after infection after propidium iodide staining and FACS analysis. Results are representative of three independent experiments (\*\**P* < 0.01, compared with G<sub>2</sub>/M of HXO-RB<sub>44</sub> treated with PBS or AdGFP).



**Infection and Replication of H101 in Retinoblastoma Tumors**

To determine infection and replication of the H101 virus in retinoblastoma tumors *in vivo*, we performed immunohistochemistry for adenoviral fiber protein on paraffin-embedded tissue sections of retinoblastoma xenografts. Tumors were harvested on day 7 after four injections of H101, AdGFP, or

PBS. As seen in Figure 8A, more adenoviral particles were detected in tumors in the H101-treated group (23.37% adenoviral-positive HXO-RB<sub>44</sub> cells) than in the AdGFP group (1.83% adenoviral-positive HXO-RB<sub>44</sub> cells) or the PBS group (0.01% adenoviral-positive HXO-RB<sub>44</sub> cells). There was almost no adenovirus particle (0.01% adenoviral positive HXO-RB<sub>44</sub> cells) in neighboring muscle, muscle, kidney, liver, heart, lung, and spleen in the H101-treated group (Fig.

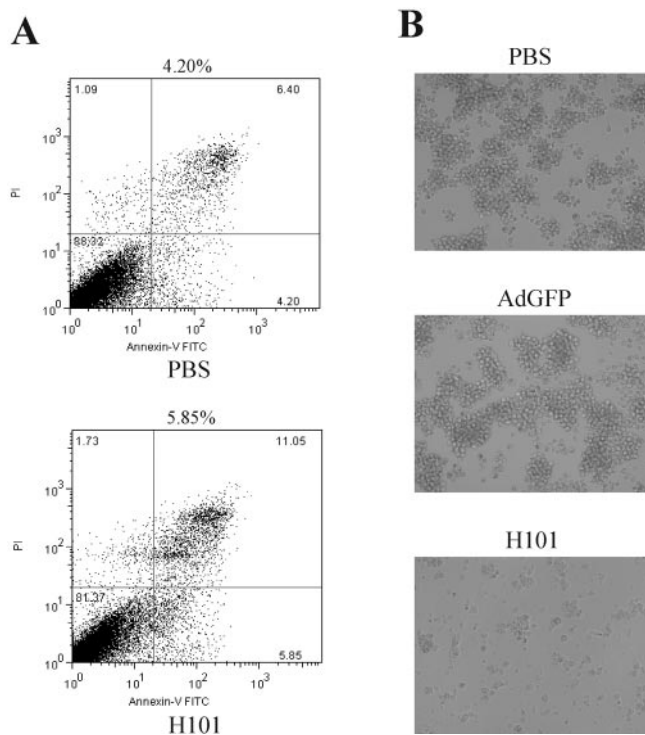


**FIGURE 6.** Detection of apoptosis and cytolysis in H101-treated HXO-RB<sub>44</sub> cells. (A) Apoptosis was measured by flow cytometric analysis at 24 hours after treatment of H101 and PBS. (B) H101 induced HXO-RB<sub>44</sub> lysis on day 5. Original magnification,  $\times 200$ .

8B), suggesting that H101 is locally replicated in tumors that lack the activity of *p53* and will not replicate in other tissues with normal *p53* activity.

Similarly, Western blot analysis showed a clear increment of adenovirus Hexon protein in the H101-treated group compared with the viral control (Fig. 8C). Taken together, these data indicate that H101 infects and replicates effectively in retinoblastoma tumors, whereas normal cells are not affected.

## DISCUSSION

Oncolytic viruses present an exciting new treatment modality in cancer therapy. In the present study, we examined the effectiveness of conditionally replicating oncolytic adenovirus H101 in the treatment of retinoblastoma in vitro and in vivo. The results indicate that H101 inhibits retinoblastoma tumor growth (Fig. 7A) and prolongs survival in animals bearing retinoblastoma tumors (Fig. 7B).

Local chemoreduction for intraocular retinoblastoma is being studied to find ways to avoid the toxicity of systemic chemotherapy. One local chemoreduction approach is subconjunctival injection of chemotherapeutic drugs. Subconjunctival injections of carboplatin in humans induce retinoblastoma regression within 3 to 4 weeks, but the response might not be long term.<sup>21</sup> Overexpression of P-glycoprotein is considered to be a major cause of drug resistance and is a serious obstacle in cancer treatment.<sup>22</sup> Gene therapy is another approach to induce local chemoreduction. Oncolytic virus replication leads to amplification of the viral input "dose" through viral release by virus-mediated lysis of the infected cells and the subsequent spread and infection of surrounding cells. H101, in combination with chemotherapy, is effective in the treatment of patients with late-stage cancers, including squamous carcinoma and esophageal, gastric, lung, colorectal, and breast cancers.<sup>23</sup>

We now show that H101 is an effective therapy in the retinoblastoma model.

H101 is a replication-selective human type-5 adenovirus lacking the 55-kDa viral gene *E1B*, the product of which is required to inactivate the cellular tumor suppressor *p53*. Activated *p53* in cells prevents efficient viral replication in normal cells. Thus, cancer cells lacking functional *p53* might be sensitive to viral replication and subsequent cytopathic effects. Dysfunctional tumor suppressor genes such as *p53* are the most common genetic lesions identified in human cancers cells, which is why H101 can be used for cancer gene therapy. Although *p53* protein is highly expressed in retinoblastoma,<sup>24</sup> the loss of heterozygosity in the *VNTR* region of intron 1 of *p53* is detected in 2 of 10 retinoblastoma cases.<sup>25</sup> Moreover, retinoblastoma has *MDMX* gene amplifications that inactivate the *p53* pathway by reducing steady state amounts of the *p53* protein,<sup>18</sup> accounting for the loss of *p53* function in patients with retinoblastoma.<sup>19</sup>

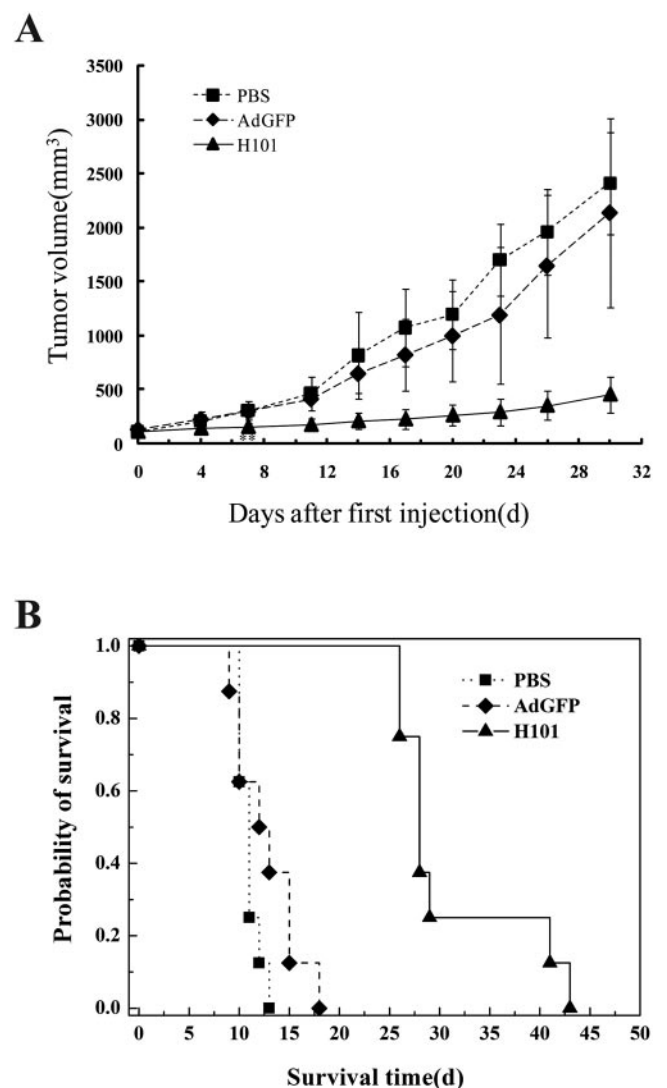


**FIGURE 7.** H101 inhibited tumor growth in vivo and prolonged mouse survival. HXO-RB<sub>44</sub> cells were injected into the right flanks of NOD-SCID mice. Animals bearing tumors of 100 to 200 mm<sup>3</sup> were treated with H101, AdGFP, or PBS. (A) Tumor growth curves (8 mice/group). Data are expressed as mean  $\pm$  SD (\*\**P* < 0.01, compared with tumor volume of PBS group). (B) Animal survival as a function of time after treatment was analyzed by Kaplan-Meier survival analysis (8 mice/group).

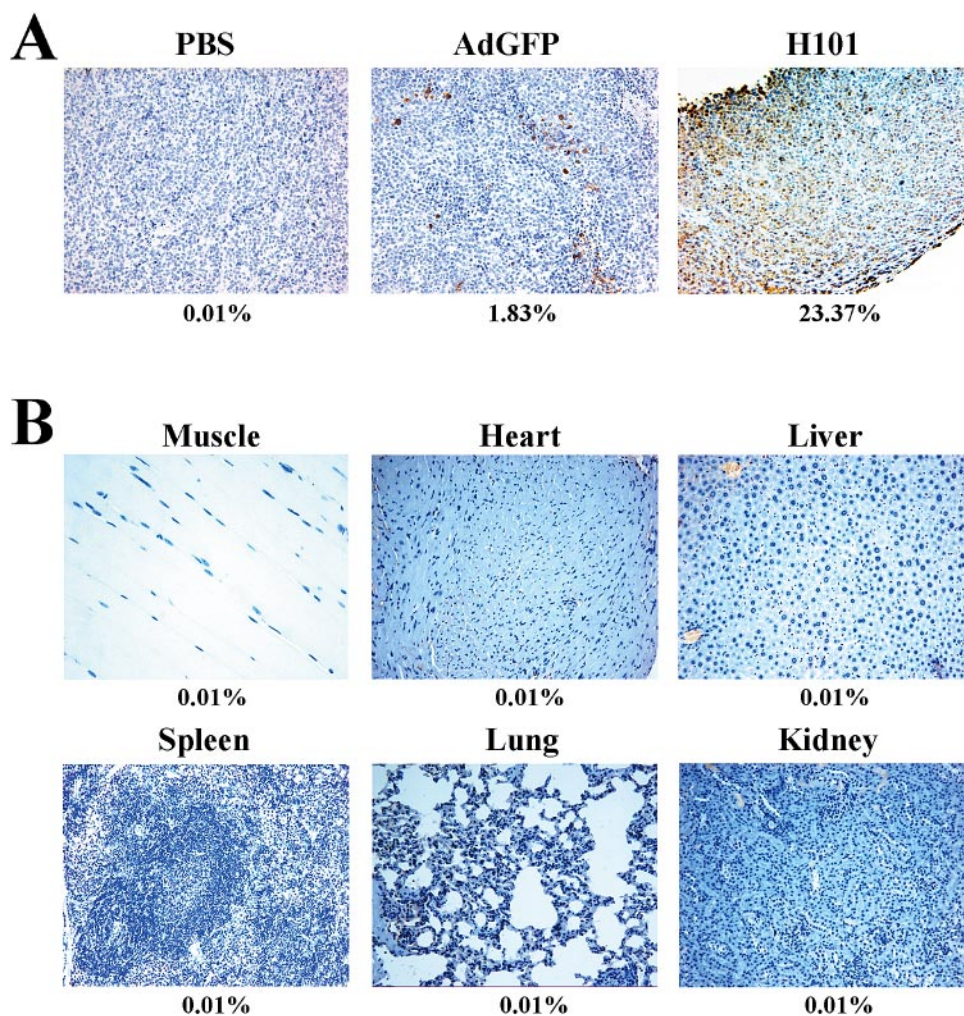


**FIGURE 8.** H101 replication in human retinoblastoma xenografts. The spread of adenovirus type 5 particles in tumors was determined by immunohistochemical detection using anti-adenoviral fiber antibody. **(A)** Adenovirus type 5 particles in RB xenografts of PBS group, AdGFP group, and H101 group collected on day 7 of the last viral injection. HXO-RB<sub>44</sub> cells infected by adenovirus type 5 particles were quantitated, and the percentage was calculated for each treatment group. Original magnification,  $\times 200$ . **(B)** Undetectable adenovirus type 5 particles in different organs in the H101 group. Original magnification,  $\times 200$ . **(C)** Western blot analysis of Hexon protein expression in retinoblastoma xenografts on day 14.

CAR has been identified as a cellular receptor for adenovirus group C serotypes 2 and 5 (AdV2, AdV5) fibers and for Coxsackie B virus, and it is very important for attachment of the adenovirus to the cells.<sup>26,27</sup> Mallam et al.<sup>28</sup> demonstrated that more than 90% of retinoblastoma cells expressed CAR and CD46, another adenovirus receptor, by immunohistochemistry and flow cytometry. RT-PCR in the present study also clearly indicated that HXO-RB<sub>44</sub> cell lines express the CAR gene. CAR protein expression was verified by Western blot analysis, im-

munocytochemistry, and immunofluorescence (Figs. 2B-D). Thus, retinoblastoma seems to be a tumor that is well suited for H101 gene therapy.

We next verified that the retinoblastoma cell lines are sensitive to treatment with H101. As demonstrated in Figure 2E, the infection efficiency of HXO-RB<sub>44</sub> was 82% at an MOI of 100. The transduction efficiency of the adenovirus in retinoblastoma was higher than that in the Y79 cell line.<sup>28</sup> Our findings indicate that H101 strongly induced retinoblastoma cell death

in vitro with an obvious dose-time effect. Nearly 80% of HXO-RB<sub>44</sub> cell were killed on day 5 after infection at an MOI of 100 (Figs. 3A, 3B). Retinoblastoma cell death is caused by lysis directly rather than by apoptosis (Fig. 6). These data demonstrate that H101 is effective against retinoblastoma in vitro and is suitable for further in vivo experiments.

Based on the in vitro results, we investigated the therapeutic effects of H101 on tumor growth of SC HXO-RB<sub>44</sub> cell xenografts. In vivo experiments indicated that intratumoral injection of H101 inhibited retinoblastoma tumor growth in NOD-SCID mice. Tumor volume did not increase for a long period afterward (Fig. 7A). No observable toxicities were noted in the H101 treatment group compared with the control group with respect to weight and general behavior.

It should be emphasized that the xenograft model used in this study may vary from retinoblastoma tumors in patients. Thus, these data might not directly translate to human studies. However, we observed antitumor activity similar to that reported in other tumor models.<sup>29,30</sup> We predict that the antitumor efficacy may be potentiated by combining H101 with other local therapeutics. Recently, we demonstrated the enhanced antitumor effect of H101 in combination with a *Bcl2* RNAi that targets the overexpressed oncogene in tumors.<sup>20</sup> In an extended study, we also proved that combined therapy of radiation with a modified H101 adenovirus that contains the Egr-1/TRAIL expression cassette significantly killed cervical tumor cells (Wang H, et al., unpublished data, 2010). We predict that H101 may be more effective in treating retinoblastomas when combined with existing clinical therapies.

Selective replication of H101 in tumors was further evaluated by measuring quantitative viral yields in treated cells using real-time PCR and end point dilution titration of HEK293 cells. To eliminate interference from the leftover H101 from the previous viral injection, we extended tumor tissue collection to 7 days after the final viral injection. We checked adenoviral fiber protein with immunohistochemistry (Figs. 8A, 8B). Very few viral particles were detected in AdGFP controls in which adenovirus was incapable of replicating in tumor cells. However, adenovirus particles distributed extensively in tumors treated with H101, which was conditionally replicated. At day 7, the extent of H101 spread in tumor increased significantly compared with day 5 tumors, implying continuous replication of H101 in tumors.

To further verify viral replication, adenoviral Hexon protein was measured by Western blot on day 14. Similarly, higher levels of adenovirus Hexon protein in the H101-treated group were compared with the AdGFP controls (Fig. 8C). Taken together, these data indicate that H101 infects and replicates selectively in retinoblastoma tumors. By immunohistochemical staining, we did not find systematic H101 spreading and replication into neighboring tissues, suggesting that H101 is a safe antitumor agent (Fig. 8B).

The mechanism underlying tumor-specific killing by the conditionally replicated adenovirus has been extensively studied in a variety of tumor models. We also conducted some mechanistic work to delineate how H101 selectively kills retinoblastoma cells. As shown in Figures 5 and 6, we demonstrated that the observed tumor cell killing and growth inhibition are related primarily to direct tumor lysis from the H101 virus rather than through activation of the cell apoptosis pathway. Tumor cell lysis and the subsequent inhibition of tumor growth are probably caused by cell arrest in the G<sub>2</sub>/M phase of HXO-RB<sub>44</sub> cells by H101. These data are consistent with the report on ONYX015 by Cherubini.<sup>31</sup> It is known that the *p53* pathway is inactivated in most retinoblastoma patients because of the overexpressed *MDM2* and *MDMX* genes.<sup>19</sup> Thus, H101 may inhibit retinoblastoma growth by the same oncolytic

mechanism that targets *p53* inactivation in tumors. Further studies are needed to address this hypothesis.

Compared with the recent chemotherapeutics applied in retinoblastoma, H101 has the following advantages. First, the safety of H101 therapy has been demonstrated in tumor patients.<sup>23</sup> Local rejection avoids the toxicity of systemic chemotherapy. Intravitreal injection techniques modified from a transcorneal approach were used safely in retinoblastoma patients with vitreous tumor seeds, and no tumor seeding along the needle tract was detected. Only mild to moderate local inflammation was observed in patients after the intraocular injection of the adenovirus.<sup>32</sup> Second, there is no predicted drug resistance. H101 may overcome the drawback of drug resistance common to many chemotherapeutics because of its unique tumor-specific lysis. Third, H101 is suitable for patients with vitreous seeds. A recent phase I study using suicide gene therapy demonstrated durable clinical and histopathologic responses in patients with vitreous seeds.<sup>32</sup> Because of the selective replication in tumor cells, we expect that H101 may be effective against vitreous seeding. In future experiments, we will test the antitumor activity of H101 combined with brachytherapy in a retinoblastoma orthotopic implantation model.

There is always a concern of the host immune response that results in the reduced efficacy of the virotherapy. Improved tumor therapy can be achieved by sustaining adenoviral replication using immunosuppression.<sup>33</sup> However, the fact that immune privilege exists within the eye<sup>34,35</sup> may actually be an advantage for retinoblastoma virotherapy. H101 may easily escape from immune surveillance, resulting in enhanced spread of viral infection and tumor lysis. On the other hand, viral lysis may activate the host immune response to attack virally infected tumor cells, thus benefiting patients who have had H101 therapy.

In summary, H101 inhibits retinoblastoma tumor growth and prolongs tumor survival in mice. This study may add H101 oncolytic adenovirus as a new therapeutic alternative for the treatment of retinoblastoma.

## References

1. Devesa SS. The incidence of retinoblastoma. *Am J Ophthalmol.* 1975;80:263-265.
2. Shields CL, Shields JA. Diagnosis and management of retinoblastoma. *Cancer Control.* 2004;11:317-327.
3. Broaddus E, Topham A, Singh AD. Incidence of retinoblastoma in the United States: 1975-2004. *Br J Ophthalmol.* 2009;93:21-23.
4. Abramson DH, Scheffer AC. Update on retinoblastoma. *Retina.* 2004;24:828-848.
5. Byrne J, Fears TR, Whitney C, et al. Survival after retinoblastoma: long-term consequences and family history of cancer. *Med Pediatr Oncol.* 1995;24:160-165.
6. Melamud A, Palekar R, Singh A. Retinoblastoma. *Am Fam Physician.* 2006;73:1039-1044.
7. Uusitalo MS, Van Quill KR, Scott IU, Matthay KK, Murray TG, O'Brien JM. Evaluation of chemoprophylaxis in patients with unilateral retinoblastoma with high-risk features on histopathologic examination. *Arch Ophthalmol.* 2001;119:41-48.
8. Honavar SG, Singh AD, Shields CL, et al. Postenucleation adjuvant therapy in high-risk retinoblastoma. *Arch Ophthalmol.* 2002;120:923-931.
9. Chintagumpala M, Chevez-Barríos P, Paysse EA, Plon SE, Hurwitz R. Retinoblastoma: review of current management. *Oncologist.* 2007;12:1237-1246.
10. Bischoff JR, Kim DH, Williams A, et al. An adenovirus mutant that replicates selectively in *p53*-deficient human tumor cells. *Science.* 1996;274:373-376.
11. Ries S, Korn WM. ONYX-015: mechanisms of action and clinical potential of a replication-selective adenovirus. *Br J Cancer.* 2002;86:5-11.

12. Wiman KG. Strategies for therapeutic targeting of the p53 pathway in cancer. *Cell Death Differ*. 2006;13:921-926.
13. Post LE. Selectively replicating adenoviruses for cancer therapy: an update on clinical development. *Curr Opin Invest Drugs*. 2002;3:1768-1772.
14. Yu W, Fang H. Clinical trials with oncolytic adenovirus in China. *Curr Cancer Drug Targets*. 2007;7:141-148.
15. Kasuya H, Takeda S, Shimoyama S, et al. Oncolytic virus therapy-foreword. *Curr Cancer Drug Targets*. 2007;7:123-125.
16. Olivier M, Eeles R, Hollstein M, et al. The IARC Tp53 database: new online mutation analysis and recommendations to users. *Hum Mutat*. 2002;19:607-614.
17. Laurie NA, Donovan SL, Shih CS, et al. Inactivation of the p53 pathway in retinoblastoma. *Nature*. 2006;444:61-66.
18. Marine JC, Dyer MA, Jochemsen AG. MDMX: from bench to bedside. *J Cell Sci*. 2007;120:371-378.
19. Laurie NA, Shih CS, Dyer MA. Targeting MDM2 and MDMX in retinoblastoma: targeting MDM2 and MDMX in retinoblastoma. *Curr Cancer Drug Targets*. 2007;7:689-695.
20. Zhang H, Wang H, Zhang J, et al. Enhanced therapeutic efficacy by simultaneously targeting two genetic defects in tumors. *Mol Ther*. 2009;17:57-64.
21. Abramson DH, Frank CM, Dunkel IJ. A phase I/II study of subconjunctival carboplatin for intraocular retinoblastoma. *Ophthalmology*. 1999;106:1947-1950.
22. Elsinga PH, Hendrikse NH, Bart J, et al. PET studies on P-glycoprotein function in the blood-brain barrier: how it affects uptake and binding of drugs within the CNS. *Curr Pharm Des*. 2004;10:1493-1503.
23. Lu W, Zheng S, Li XF, Huang JJ, Zheng X, Li Z. Intra-tumor injection of H101, a recombinant adenovirus, in combination with chemotherapy in patients with advanced cancers: a pilot phase II clinical trial. *World J Gastroenterol*. 2004;10:3634-3638.
24. Yuge K, Nakajima M, Uemura Y, Miki H, Uyama M, Tsubura A. Immunohistochemical features of the human retina and retinoblastoma. *Virchows Arch*. 1995;426:571-575.
25. Emre S, Sungur A, Bilgic S, et al. Loss of heterozygosity in the VNTR region of intron 1 of p53 in two retinoblastoma cases. *Pediatr Hematol Oncol*. 1996;13:253-256.
26. Bergelson JM, Modlin JF, Wieland-Alter W, et al. Clinical coxsackievirus B isolates differ from laboratory strains in their interaction with two cell surface receptors. *J Infect Dis*. 1997;175:697-700.
27. Tomko RP, Xu R, Philipson L. HCAR and MCAR: the human and mouse cellular receptors for subgroup C adenoviruses and group B coxsackieviruses. *Proc Natl Acad Sci USA*. 1997;94:3352-3356.
28. Mallam JN, Hurwitz MY, Mahoney T, Chévez-Barrios P, Hurwitz RL. Efficient gene transfer into retinal cells using adenoviral vectors: dependence on receptor expression. *Invest Ophthalmol Vis Sci*. 2004;45:1680-1687.
29. He XP, Su CQ, Wang XH, et al. E1B-55kD-deleted oncolytic adenovirus armed with canstatin gene yields an enhanced antitumor efficacy on pancreatic cancer. *Cancer Lett*. 2009;285:89-98.
30. Kim J, Kim PH, Yoo JY, et al. Double E1B 19 kDa- and E1B 55 kDa-deleted oncolytic adenovirus in combination with radiotherapy elicits an enhanced antitumor effect. *Gene Ther*. 2009;16:1111-1121.
31. Cherubini G, Petouchoff T, Grossi M, Piersanti S, Cundari E, Saggio I. E1B55K-deleted adenovirus (ONYX-015) overrides G1/S and G2/M checkpoints and causes mitotic catastrophe and endoreduplication in p53-proficient normal cells. *Cell Cycle*. 2006;5:2244-2252.
32. Chevez-Barrios P, Chintagumpala M, Mieler W, et al. Response of retinoblastoma with vitreous tumor seeding to adenovirus-mediated delivery of thymidine kinase followed by ganciclovir. *J Clin Oncol*. 2005;23:7927-7935.
33. Thomas MA, Spencer JF, Toth K, Sagartz JE, Phillips NJ, Wold WS. Immunosuppression enhances oncolytic adenovirus replication and antitumor efficacy in the Syrian hamster model. *Mol Ther*. 2008;16:1665-1673.
34. Niederkorn JY. Immune escape mechanisms of intraocular tumors. *Prog Retin Eye Res*. 2009;28:329-347.
35. Niederkorn JY. Mechanisms of immune privilege in the eye and hair follicle. *J Invest Dermatol Symp Proc*. 2003;8:168-172.